Performance of Reinforced Subbase Materials by Geogrid as Abase Layer Under Weak Subgrade

Qais S. Banyhussan[1,a], Hanan A. hassan[1,b], and Ali J. Kadhum[1,c*]

[1]Highway and Transportation Department, Mustansiriyah University, Baghdad, Iraq

[a]qaisalmusawi@uomustansiriyah.edu.iq, [b]ghassan_hanan@uomustansiriyah.edu.iq, and

[c]edma028@uomustansiriyah.edu.iq

*Corresponding author

Abstract. The current study examines how an unpaved road behaves when it is installed on top of a soft clay layer that's been strengthened at the subgrade/subbase interface with a single layer of geogrid type SS2 is used to reinforce a laboratory model, and cycling load is used to apply repeated loads to the model. Subbases with and without reinforcement over soft subgrade were built in a sizable test box. (1000 mm×1000 mm×1000 mm). The test results show that using a geogrid reinforcement layer enhances the number of cycles and stress distribution while decreasing displacement on the soft subgrade surface on reinforced models compared to similar unreinforced ones for the same rutting value (85 mm). The rate of increase in failure time is about (6.12, 3.7, and 1.7) for 150, 230, and 300 mm thickness, respectively. The rate of redaction in vertical stress is about (18, 12.5, and 7.1) % for 150 mm, 230 mm, and 300 mm thickness, respectively.

Keywords: Geogrid; vertical stress; subbase; cyclic load; LVDT.

1. INTRODUCTION

Pavements with weak subgrades are supported by an aggregate base course layer, which, when combined with geosynthetics, improves the pavement's performance by raising the base aggregate's elastic modulus, enhancing the stress distribution within the subgrade, minimizing lateral movement of the base aggregate, minimizing shear strains at the top of the subgrade, raising the pavement section's bearing capacity, and lengthening the service life [1-4]. The main purposes of geosynthetics in the design of pavement are subgrade stabilization and separation, base reinforcement, and filtration or drainage. Numerous academics have investigated the idea of adding a reinforcing geosynthetic layer to the subbase/base granular material of an unpaved road system throughout the last three to four decades. The full-scale test is how experimental research is carried out [5-6]. Laboratory plate loading testing in a big test box [7-9] and laboratory or field tests to evaluate the effectiveness of geosynthetic reinforcement under field conditions. Unpaved roads have two layers: natural subgrade and subbase course. The soil that makes up the current subgrade is frequently too weak to handle the traffic loads. Traditional approaches to dealing with soft subgrade soils include removing the weak soil and replacing it with strong fill material, using thick pavement sections to distribute vertical loads over a large area of the subgrade, and chemically stabilizing or modifying the subgrade with calcium-based materials that increase strength and bearing capacity (e.g., cement, lime, fly ash).

A growing component of pavement system design and repair is the use of innovative technologies to improve pavement performance and service life. Numerous solutions have been proposed over the last three decades as systems that could improve pavement performance and stop current premature failures [10-15]. This study looks into the performance enhancement of an unpaved road that has been reinforced with a single layer of geogrid put at the soft subgrade/subbase interface and exposed to repetitive loading.

In this work, three subbase layer thicknesses—150 mm, 230 mm, and 300 mm—were used in a total of six model experiments that represent two series: The first series consists of three models with h=150, 230, and 300 mm, where h is the thickness of the subbase layer. One model in this series is unreinforced, and the other three models are reinforced with SS2 geogrid. The study's objective was to determine how the geogrid reinforcement layer, compared to an unreinforced section, affected the depth of ruts and the distribution of stress at the subbase-subgrade interface.

2. MATERIAL USED

2.1 Subgrade Soil

The clay soil employed as a subgrade material in this investigation was brought from the Al_Tajiyat area north of Baghdad. Figure 1 shows the grain size distribution curve of subgrade material. The soil was classified as (CL) based on (ASTM D4318, 2010) and (A-6) according to the AASHTO. The physical and chemical properties of the clay soil employed in this study are listed in Table 1. The modified proctor test was performed on clay soil to identify the maximum dry density and optimal moisture content for the test, as shown in Figure

2. According to the result of CBR variation with water content shown in Figure 3, the soil was prepared at CBR (2%) in a manufactured box corresponding to a water content of (20%).

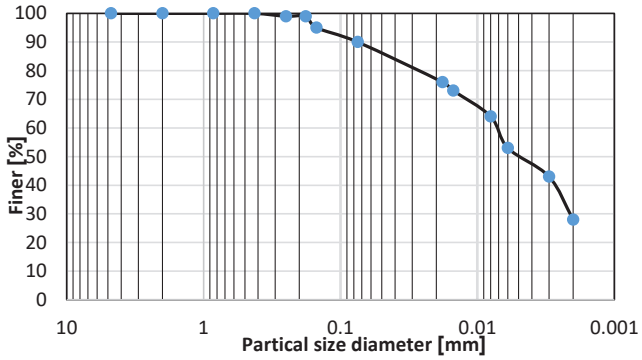

Figure 1: Grain size distribution curve of clay soil.

Table 1: Physical and chemical properties of clay soil used in the study.

Material Properties	Values	Standards
Specific gravity	2.68	ASTM D 854 (2014)
Liquid limit (%)	40	ASTM D 4318 (2017)
Plastic limit (%)	14	ASTM D 4318 (2017)
Plasticity index (%)	26	ASTM D 4318 (2017)
Maximum dry density (g/cm^3)	1.78	ASTM D 1557-07
Optimum moisture content (%)	10.2	ASTM D 1557-07
CBR with 95% compaction	5	
Organic matter, %	1.89	(SCRB/R6,2003) (2 max)
T.S.S (%)	4.61	(SCRB/R6,2003) (10 max)
SO3 content (%)	1.64	(SCRB/R6,2003) (5 max)
Gypsum content (%)	3.52	(SCRB/R6,2003) (10.75 max)
Soil classification	A-6	AASHTO
Unified soil classification	CL	ASTM D-2487 (2017)

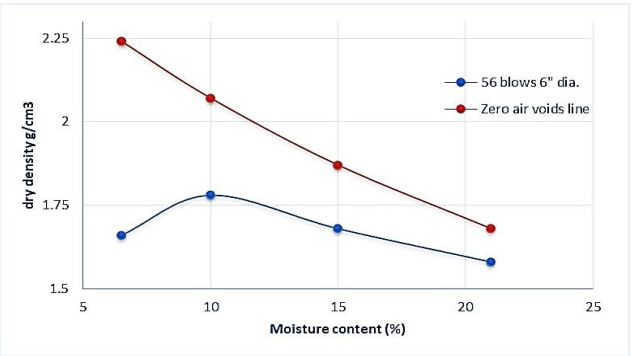

Figure 2: Compaction curve of subgrade soil.

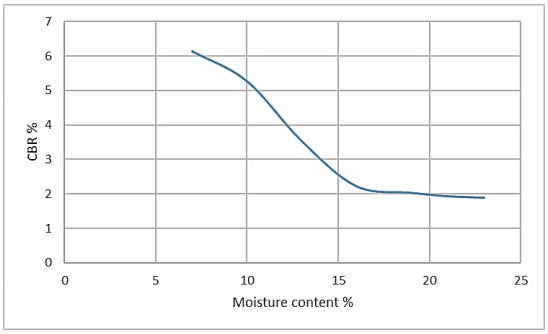

Figure 3: Variation of CBR with water content.

2.2 Subbase

Subbase Type B was collected from the AL-Niba'ee region north of Baghdad to be used in this study. Table 2 shows the results of both chemical and physical tests on the subbase material. Figure 4 and Table 3 show the gradation and sieve analysis of the subbase material according to the permitted limits of the Iraqi specification (R6).

Table 2: Physical and chemical properties of the subbase material.

Type of test	Results	standards
Liquid limit (%)	21	ASTM D 4318 (2017)
Plastic limit (%)	0	ASTM D 4318 (2017)
Plasticity index (%)	N	ASTM D 4318 (2017)
Specific gravity	2.58	ASTM D-854-14
Maximum dry density (g/cm^3)	2.198	ASTM D 1557-07
Optimum moisture content (%)	6.8	ASTM D 2216
C.B.R at 95% compaction	40	ASTM D 1883
Organic matter (%)	1.8	(SCRB/R6,2003) (2 max)
T.S.S (%)	7	(SCRB/R6,2003) (10 max)
SO3 content (%)	4.1	(SCRB/R6,2003) (5 max)
Gypsum content (%)	8.815	(SCRB/R6,2003) (10.75 max)
Classification of subbase	GW-GM	USCS

Table 3: Iraqi specification of the subbase material (SORB, 1983 - R6).

Sieve size (mm)	Iraqi standards for passing Type B %	Subbase passing %
50	100	100
25	75-95	100
9.5	40-75	63.4
4.75	30-60	40.46
2.36	21-47	34.43
0.3	14-28	20.76
0.075	5-15	1.96

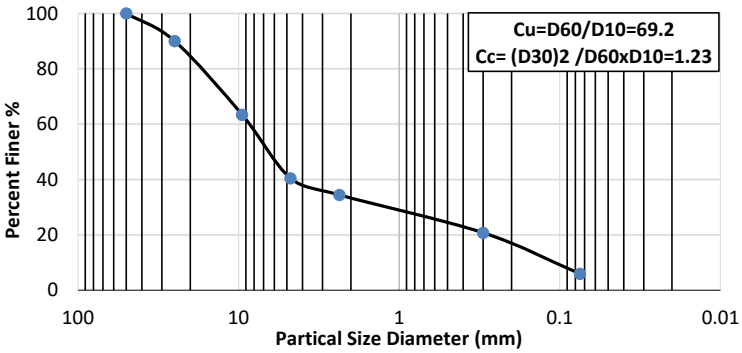

Figure 4: Grain size analysis curve of subbase.

2.3 Geosynthetics

2.3.1 Geogrid

The geogrid employed in this study was SS2, as shown in Figure 5, and was manufactured by QMOF Company (Quality Material of Oil Field) [16]. The physical and mechanical parameters of the geogrid type SS2 are shown in Table 4.

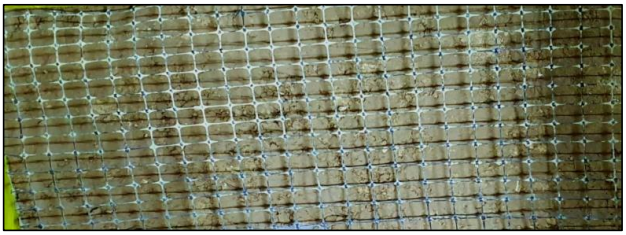

Figure 5:Geogrid type SS2 reinforcement.

Table 4: Physical and mechanical properties of geogrid.

The physical properties	**Data**	
Polymer	Pp	
color	Black	
Polymer type	SS2	
Rib shape	Rectangular	
Dimensional properties	**Unit**	**Data**
Roll width	m	4
Roll length	m	50
Unit weight	kg/m^2	0.29
Aperture size	mm	28×40
WLR	mm	3
WTR	mm	3
tLR thickness of transverse ribs	mm	0.9
tLR thickness of longitudinal ribs	mm	1.2
Load at 2% strain (3)	kN/m	7.0
Load at 5% strain (3)	kN/m	14.0
Load at 2% strain (3)	kN/m	12.0
Load at 5% strain (3)	kN/m	23.0

3. MODEL DESIGN AND MANUFACTURING

Figure 6 depicts an experimental setup designed and manufactured at a scale of about one-tenth that of the prototype. The test apparatus consists of a steel tank box (1.0 m x 1.0 m x 1.0 m). A cyclic load was applied using a 200 mm diameter circular steel plate under a hydraulic jack connected to a hydraulic system. In all tests, the frequency was set to 1 Hz. In all tests, the cyclic applied load was 20 kN, resulting in a pressure load of 552 kPa. It was a typical truck axle load simulation with a contact pressure of 552 kPa. A shaft encoder to measure the displacement in the middle of the model, displacement transducers (LVDT) to detect vertical displacements, and a programmable logic controller (PLC) to measure the loads during cyclic loadings At various points in the subgrade, a flexible force sensor and strain gauge are employed to detect the forces and strains, respectively.

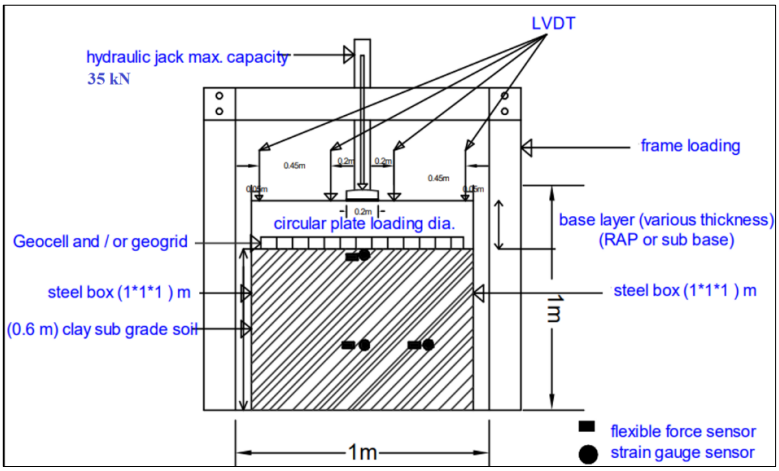

Figure 6: Model setup.

4. TEST PREPARATIONS

The subgrade soil was dried, homogeneously mixed with a moisture content of 20%, and then placed in nylon bags for 24 hours. The subgrade was then placed in the box test in 6 layers, with each layer being compressed well to reach a height of 60 cm. Each layer was compacted well by steel tamping (10x20) cm. After it had been prepared, three strain gauges and three force sensors were installed on the center and sides of the subgrade. A steel beam fixed a four (LVDT) above the box to detect displacement while being loaded. The geogrid was positioned on top of the subgrade for the reinforced sections following the installation of the sensors, as shown in Figure 7. The base course thickness was adjusted based on the test sections (15 cm, 23 cm, and 30 cm). Repeated plate load tests were performed on the base in both its reinforced and unreinforced states. The LVDT was positioned on the sample and connected with a data logger and computer, is shown in Figure 8.

Figure 7: Preparation model.

Figure 8: Sample during the test.

5. RESULT AND DISCUSSION

The failure criteria used in this study are 85 mm permanent deformation in the center of the base layer or when 1000 cycles are reached, whichever is more likely. This study carried out six tests, with and without reinforcement, three reinforced tests with geogrid, and three unreinforced. The interface between the subgrade and the subbase was reinforced.

5.1 Displacement – Time Relationship for the Model Tests

In unreinforced models, the vertical displacement of the unpaved layers is measured at the surface of the subbase layer. All unreinforced tests of three samples of 15 cm, 23 cm, and 30 cm thickness failed. A typical relationship between displacement and loading cycles is presented in Figure 9, showing that displacement increased with the increasing number of cycles, and this matches what he found [17]. And this thing is self-evident since the base layer is stronger than the subgrade layer. For the reinforced models, the vertical displacement of the unpaved layers is measured at the surface of the subbase layer. From Figure 10, it is noticed that the model needs more cycles, i.e., a longer time when the thickness of the base layer is increased, In addition to the above, the models reinforced with the geogrid layer showed our improvement clearly, as the 150 mm subbase model lasted 80 seconds, while the reinforced model lasted approximately 600 seconds, while the unreinforced 230 mm subbase model lasted 170 seconds, while the reinforced model lasted 800 seconds, and the reinforced model 300 mm subbase lost 370 seconds, and the reinforced model gave a displacement of 65 mm for a period of 1000 seconds. [18] demonstrated how shear contact between the aggregate and the geogrid during the base's attempt to extend laterally is made possible by the presence of one or more geogrid layers at the base's bottom. The geogrid was put in tension by the shear load that was transferred from the base aggregate. The geogrid's comparatively high stiffness worked to prevent lateral tensile strain from developing in the base next to the geogrid. Geogrids can improve the performance of a

pavement segment built on a low CBR subgrade, which matches with [17].The full-scale pavement test findings from the University of Illinois clearly demonstrated the performance advantages of employing geogrids, particularly in the decreased horizontal base course motions. One of the main goals of the geogrid reinforcement, which disperses load over a vast area, is to flatten the distorted shape of the subgrade, which is related to a more uniformly distributed stress on the subgrade surface.

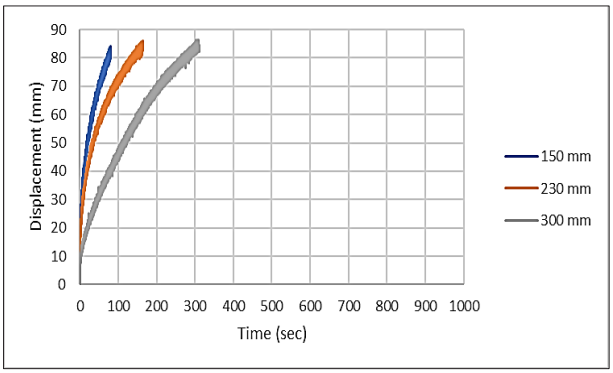

Figure 9: Displacement – time relationship for (150, 230, 300) mm unreinforced subbase thickness.

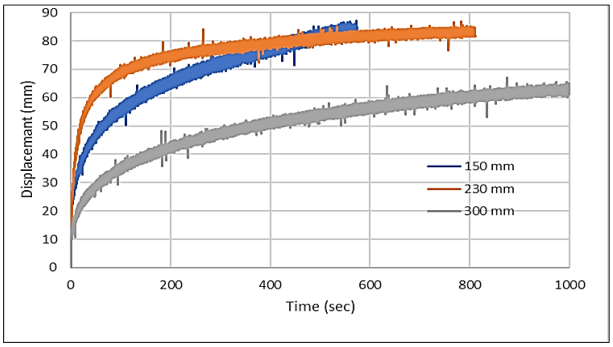

Figure 10: Displacement – time relationship for (150, 230, 300) mm reinforced subbase thickness with geogrid.

5.2 Vertical Stress - Time Relationship for the Model Tests

5.2.1 Vertical Stress - Time Relationship for Unreinforced Model

From Figures 11 to 13, it can be shown that for unreinforced models, the vertical stress was reduced by increasing the base course layer thickness. This may be due to the degradation of the base course with repeated loading cycles. The vertical stress increases, which causes the stress distribution area to become smaller, which agrees with [16]. Due to the drop in the base course's modulus and the stress distribution reduction angle, which matches [19].

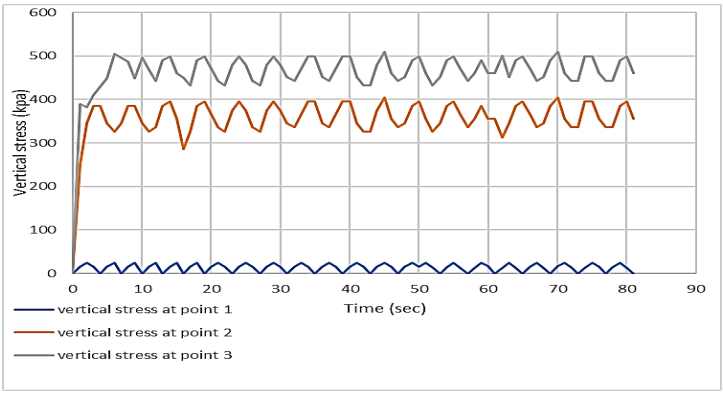

Figure 11: Vertical stress with time relationships for 150 mm subbase in the interface middle and edge.

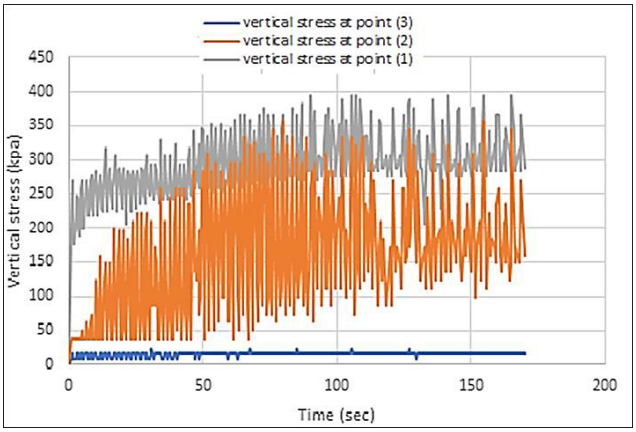

Figure 12: Vertical stress with time relationships for 230 mm subbase in the interface, middle, and edge.

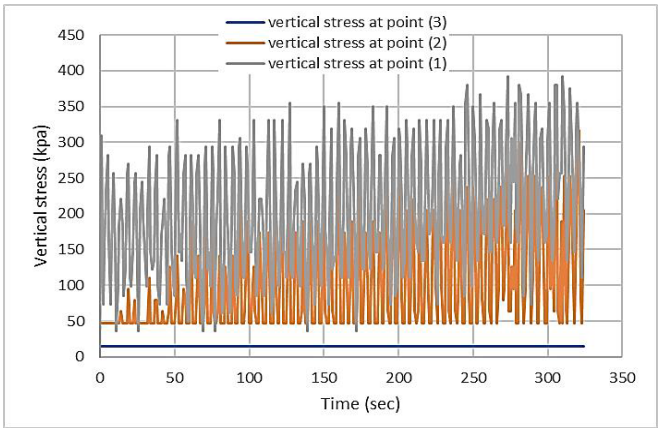

Figure 13: Vertical stress with time relationships for 300 cm subbase in the interface, middle, and edge.

5.2.2 Vertical Stress - Time Relationship for Reinforced Model

Figures 14 to 16 demonstrate that, compared to the unreinforced model, the vertical stresses decreased as the base thickness increased at around (18, 12.5, and 7.1%). This could be explained by the fact that the stress distribution angle has decreased due to the base course's degradation, which agrees with [20]. The vertical stresses may have lowered because of the improved particle geogrid interlock, consistent with [21]. Result from the creation of a stable composite between the base materials and geogrid. Because of the reorientation of the subbase particles over time, there is less interlocking at first and more over time, which is consistent with [16].

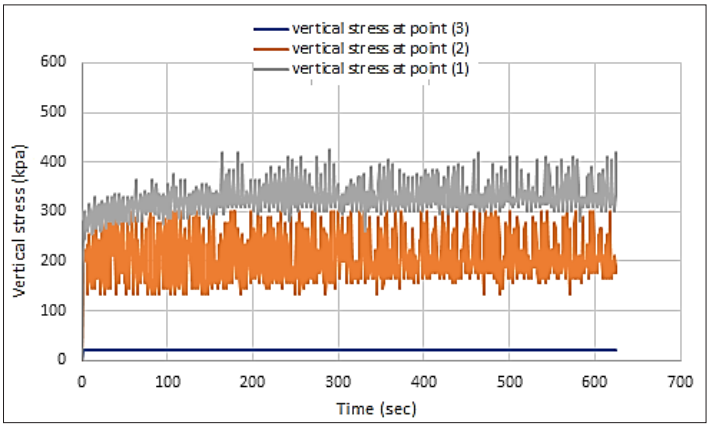

Figure 14: Vertical stress with time relationships for 150 mm subbase in the interface, middle, and edge.

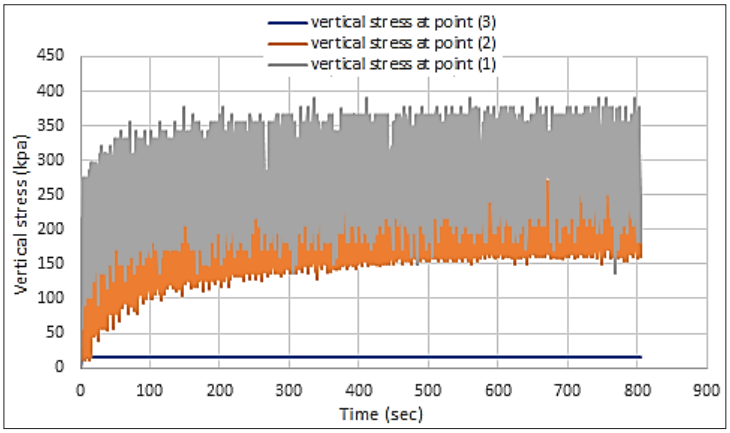

Figure 15: Vertical stress with time relationships for 230 mm subbase in the interface, middle, and edge.

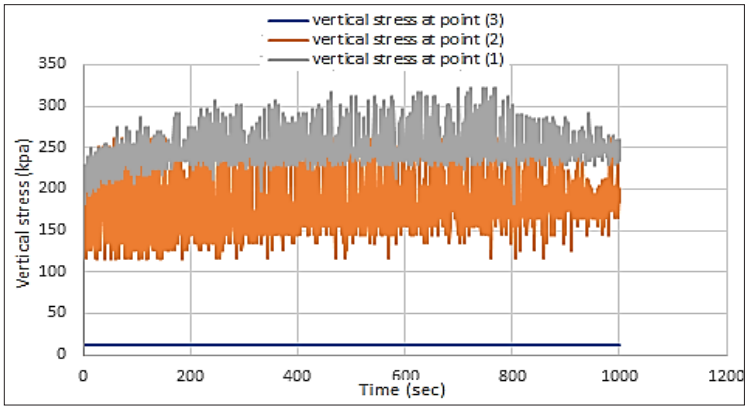

Figure 16: Vertical stress with time relationships for 300 mm subbase in the interface, middle, and edge.

5.3 Strain-Time Relationship for the Model Tests

5.3.1 Strain-time relationship for unreinforced models

From Figures 17 to 19, It can be noted that the increase in the thickness of the base layer leads to a decrease in the strain at the interface and a decrease in the strain in the middle of the subgrade, but the strain at the edge is as little as possible, and this is self-evident because the strain is distributed, the greater the thickness of the base layer, the less stress reaches the base.

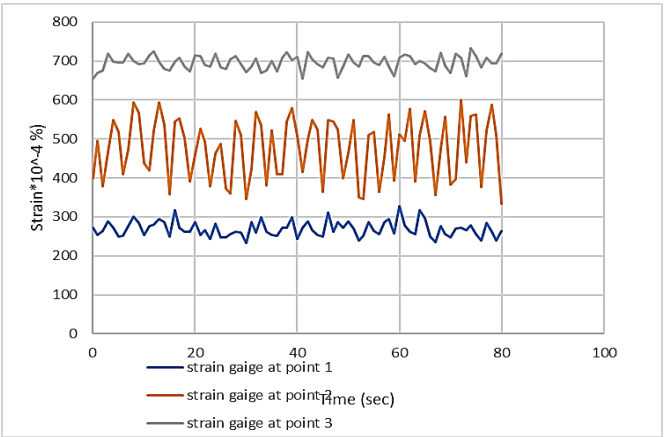

Figure 17: Strain gauge senser result for unreinforced model (150 mm subbase).

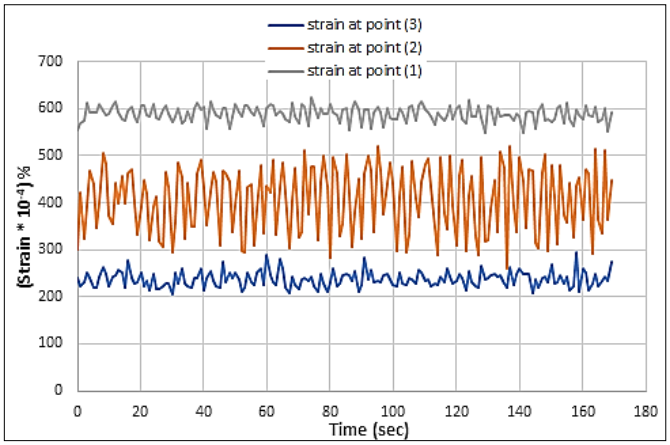

Figure 18: Strain gauge senser result for unreinforced model (230 mm subbase).

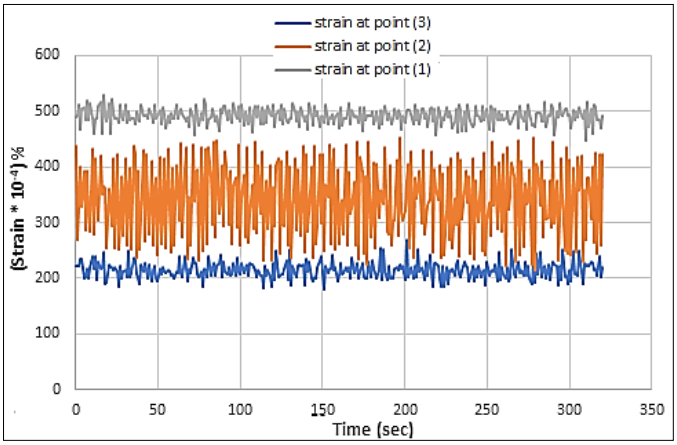

Figure 19: Strain gauge sensor result for unreinforced model (300 mm subbase).

5.3.2 Strain-time relationship for reinforced models

The relationships between strain and time are shown in Figures 20 to 22. The strain value decreases when using geogrid between the base layer and subgrade and decreases as the base layer's thickness increases. This can be attributed to a fraction of geogrid carried lateral movement and tension component. The main uses of the geogrid reinforcement, which transports loads across a large area, agree with those of [20-21].

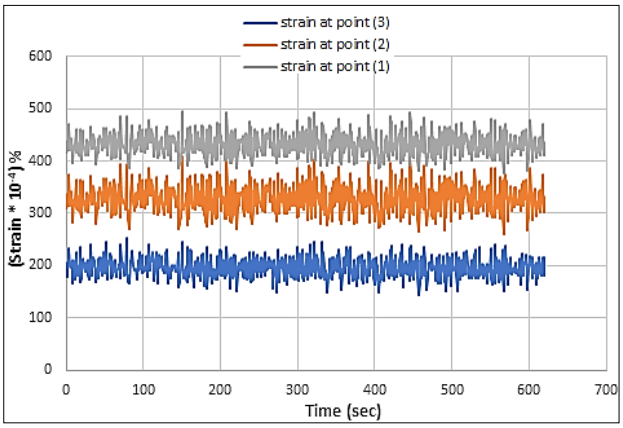

Figure 20: Strain gauge sensor result for 150 mm subbase.

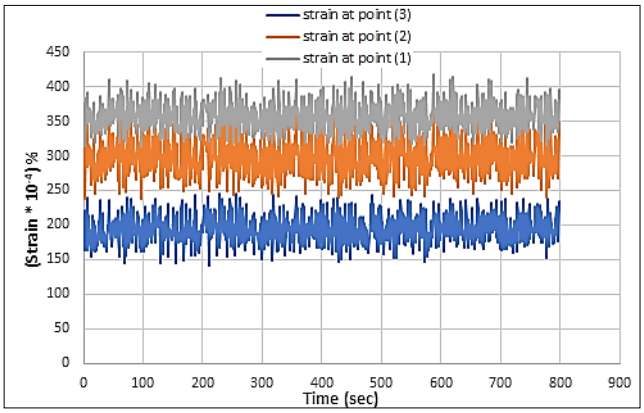

Figure 21: Strain gauge sensor result for 230 mm subbase.

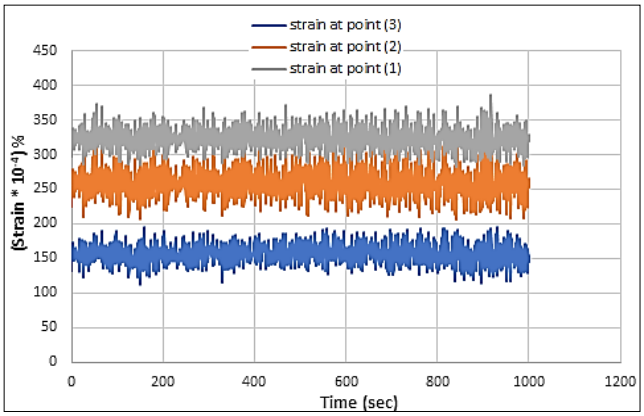

Figure 22: Strain gauge sensor result for 300 mm subbase.

6. CONCLUSIONS

The following outcomes can be deduced from repeated load tests on test sections of unsurfaced pavement reinforced with and without geogrid:

- Using geogrids can greatly enhance the performance of a pavement segment built on a low CBR subgrade.
- Increasing the subbase thickness and utilizing geogrid reinforcement both increase the number of cycles in reinforced models, with the unreinforced model experiencing an increase in cycles with the highest percentage. Adding the geogrid layer at the intersection of the subbase and subgrade results in a more flattened deformed shape on the subgrade surface, resulting in a lower displacement value for the same subbase thickness. For all models, the displacement on the subgrade surface reduces as the subbase thickness increases, with the unreinforced model showing the biggest percentage decrease.

REFERENCES

[1] Barksdale RD, Brown SF, Chan F. Potential benefits of geosynthetics in flexible pavement systems. 1989.
[2] Bathurst RJ, Karpurapu R. Large-Scale Triaxial Compression Testing of Geoceii-Reinforced Granular Soils. Geotech Test J. 1993;296–303.
[3] BETTINI V, CANCELLI C, GALANTINI R, RABITTI P, TARTAGLIA A, ZAMBRINI M. Relazione del gruppo tecnico designato dai coordinamenti delle Ammi-nistrazioni, comitati dei cittadini e associazioni ambientaliste in tutela dei territori interessati alla realizzazione delle linee ferroviarie ad alta velocità. 1996.
[4] Ling HI, Liu Z. Performance of geosynthetic-reinforced asphalt pavements. J Geotech Geoenvironmental Eng. 2001;127(2):177–84.
[5] Fannin RJ, Sigurdsson O. Field observations on stabilization of unpaved roads with geosynthetics. J Geotech Eng. 1996;122(7):544–53.
[6] Hufenus R, Rüegger R, Flum D, Sterba IJ. Strength reduction factors due to installation damage of reinforcing geosynthetics. Geotext Geomembranes. 2005;23(5):401–24.
[7] Leng J, Gabr MA. Characteristics of geogrid-reinforced aggregate under cyclic load. Transp Res Rec.

2002;1786(1):29–35.
[8] Palmeira EM, Antunes LGS. Large scale tests on geosynthetic reinforced unpaved roads subjected to surface maintenance. Geotext Geomembranes. 2010;28(6):547–58.
[9] Qian Y, Han J, Pokharel SK, Parsons RL. Experimental study on triaxial geogrid-reinforced bases over weak subgrade under cyclic loading. In: GeoFlorida 2010: Advances in Analysis, Modeling & Design. 2010.
[10] Zornberg JG, Gupta R. Reinforcement of pavements over expansive clay subgrades. In: Proceedings of the 17th International Conference on Soil Mechanics and Geotechnical Engineering (Volumes 1, 2, 3 and 4). IOS Press. 2009.
[11] Thakur JK, Han J, Pokharel SK, Parsons RL. Performance of geocell-reinforced recycled asphalt pavement (RAP) bases over weak subgrade under cyclic plate loading. Geotext Geomembranes. 2012;35(1):14–24.
[12] Rajagopal K, Chandramouli S, Parayil A, Iniyan K. Studies on geosynthetic-reinforced road pavement structures. Int J Geotech Eng. 2014;8(3):287–98.
[13] AL-Shamaa MF, Sheikha AA, Karkush MO, Jabbar MS, Al-Rumaithi AA. Numerical modeling of honeycombed geocell reinforced soil. InModern Applications of Geotechnical Engineering and Construction: Geotechnical Engineering and Construction 2021 (pp. 253-263). Springer Singapore.
[14] Karkush MO, Yassin S. Improvement of geotechnical properties of cohesive soil using crushed concrete. Civil Engineering Journal. 2019 Oct 7;5(10):2110-9.
[15] Karkush MO, Yassin SA. Using sustainable material in improvement the geotechnical properties of soft clayey soil. Journal of Engineering Science and Technology. 2020 Aug;15(4):2208-22.
[16] Jebur FF, Fattah MY, Abduljabbar AS. Function and Application of Geogrid in Flexible Pavement under Dynamic Load. Eng Technol J. 2021;39(8):1231–41.
[17] Al-Qadi IL, Brandon TL, Valentine RJ, Lacina BA, Smith TE. Laboratory evaluation of geosynthetic-reinforced pavement sections. Transp Res Rec. 1994;(1439):25–31.
[18] Fattah MY, Mahmood MR, Aswad MF. Stress distribution from railway track over geogrid reinforced ballast underlain by clay. Earthq Eng Eng Vib. 2019;18(1):77–93.
[19] Pokharel SK, Han J, Parsons RL, Qian Y, Leshchinsky D, Halahmi I. Experimental study on bearing capacity of geocell-reinforced bases. In: 8th international conference on Bearing Capacity of Roads, Railways and Airfields. Champaign, IL, USA. June 2009.
[20] Paute JL, Hornych P, Benaben JP. Repeated load triaxial testing of granular materials in the French Network of Laboratories des Ponts et Chaussées. In: Flexible Pavements Proceedings of The European Symposium Euroflex 1993 Held In Lisbon, Portugal, 20-22 September 1993. 1996.
[21] Ibrahim SF, Sofia GG, Kareem AI. Experimental study on geogrid-reinforced subbase over soft subgrade soil under repeated loading. J Eng Sustain Dev. 2012;16(3):218–40.